Correlation between CT Number shift and tissue temperature change during radiofrequency ablation: an ex-vivo study using bovine liver

IOP Conf. Series: Journal of Physics: Conf. Series **1248** (2019) 012039 doi:10.1088/1742-6596/1248/1/012039

Correlation between CT Number shift and tissue temperature change during radiofrequency ablation: an ex-vivo study using bovine liver

Dong Leng Lee[1], Yin How Wong[2], Peng Long Cheah[1], Daryl Tan[2], Kok Sing Lim[3], Azlan Che Ahmad[1], Norshazriman Sulaiman[1], Basri Johan Jeet Abdullah[1,2], Chai Hong Yeong[2]

[1]Department of Biomedical Imaging, Faculty of Medicine, University of Malaya, Kuala Lumpur, 50603, Malaysia
[2]School of Medicine, Faculty of Health and Medical Sciences, Taylor's University, Subang Jaya, 47500, Malaysia
[3]Photonics Research Centre, University of Malaya, Kuala Lumpur, 50603, Malaysia

Email: ericleedl@gmail.com

Abstract. Current post-RFA (radiofrequency ablation) evaluation of unresectable liver tumours relies on visual inspection of non-enhancing tissues on the contrasted CT (computed tomography) images. This research investigated the correlation between CT number shift (dHU) and tissue temperature change (dT) during real-time CT-guided RFA of ex-vivo bovine livers. The study aimed to develop a non-invasive CT thermometry method to guide clinicians in assessing ablation outcome. 10 liver samples were individually ablated for 12 minutes using a RFA electrode, powered by an impedance-controlled RF generator (Cool-tipTM, Metronic, USA) and subsequently cooled for 15 minutes. An optical fiber inscribed with 4 equally spaced Fiber Bragg Gratings (FBG) was inserted sideward through the liver to measure 4 temperature points at the grating positions. CT scans were performed at interval of 3 minutes from 0 to 27 minute. CT numbers at the grating positions were manually extracted, and dHU and dT were computed and plotted to investigate the relationship. From the results, CT number decreased as temperature increased during RFA, and vice versa. A negative linear relationship ($y = -0.66x + 1.23$, $R^2 = 0.925$) between dHU and dT was observed. The thermal sensitivity was determined as -0.66 ± 0.03 HU/°C. The strong correlation between dHU and dT during RFA could be used to estimate tissue temperature based on the CT number measured during real time CT-guided RFA. This approach would help the interventionalists in determining the ablation outcome hence improving treatment efficacy.

1. Introduction

When surgical resection is not possible for patients with liver, kidney, lung or bone cancers, a good alternative to treat tumour growth of 3 cm or smaller, especially for hepatocellular carcinoma (HCC) is by thermal ablation [1]. The major advantage of thermal ablation is minimally invasive and hence expedite patient's recovery. Thermal ablation of solid tumour is usually performed by interventional radiologists under the guidance of computed tomography (CT), magnetic resonance imaging (MRI) or ultrasound [2]. The ablation applicator(s) or needle(s) is inserted percutaneously to the targeted lesion and subsequently heat the tumour tissues to hyperthermia state at elevated temperature of 50°C to 100°C

[3-6] or freeze it to sub-zero temperature between -20°C to -40°C [6]. The primary aim is to heat or freeze the tumour tissues such that their proteins get denaturized and plasma membranes melted [3], ultimately achieving tumour apoptosis. The physical form of complete necrosis of tissues can be determined when the tissues coagulate into hard lump(s).

Examples of hyperthermia ablation techniques include radiofrequency ablation (RFA), microwave ablation (MWA), laser induced interstitial thermotherapy (LITT) and high intensity focus ultrasound (HIFU) [7], while cryogenic (freezing) ablation is known as cryoablation [6]. Amongst all, RFA is the most commonly practiced technique for HCC due to its ease of setup, commercial availability, lower treatment cost, higher treatment efficacy in ablating tumours parenchyma and sparring normal tissues, minimal post treatment complication and a faster recovery from the treatment wounds [5]. RFA works by transmitting alternative current of frequency at 350 – 500 kHz from a RF generator [7]. The current passes through a needle-like applicator and out to the grounding pad. As the current passes through tissues, ions within the tissues oscillate back and forth [3] between the applicator and the grounding pad, generating heat by ionic frictions among the tissue molecules near the applicator. Some commercial available RFA systems use impedance-control principle to manage the control of temperature and maximize ablation volume during the thermal ablation [3-5,8]. However, these systems lack tissue temperature monitoring capabilities and thus during CT-guided RFA, interventionalists resort to visual inspection on contrasted CT images post-RFA to determine the adequacy of ablation.

In the recent years, numerous studies on the use of contact thermometry were carried out on ex-vivo and in-vivo bovine and porcine livers to investigate the feasibility of CT thermometry using LITT [9], MWA [10,11] and RFA [12,13]. CT thermometry is a form of contactless thermometry and requires adaptation of correlation between CT number shift (dHU) and tissue temperature change (dHU) to translate CT numbers into temperatures onto the different slices of the CT images. Using this method, temperature profiles of tissues during ablation can be mapped out in real time using CT number. Invariably, it can provide a feedback tool for intervention radiologists to determine the quality and volume of tissue being ablated. CT thermometry is tissues dependence and requires contact thermometry as an initial form of calibration to determine the thermal sensitivity of the tissues concerned. Contact thermometry uses Type-K thermocouples or Fiber Bragg Grating (FBG) sensors [14,15] whereby the sensors are inserted into targeted liver sites to measure temperatures.

This study aimed to investigate the variation of CT number and temperature change during thermal ablation and cooling via RFA as well as to develop a non-invasive CT thermometry based from the obtained thermal sensitivity.

2. Methodology

2.1. Experimental Setup

Fresh bovine liver was cut and fitted into a poly(methy methacrylate) (PMMA) hollow container of 82 mm diameter x 65 mm height and placed on a stainless steel tray. Liver samples with large blood vessels were avoided as cavities of the blood vessels would result in high negative CT number and subsequently affect the accuracy of CT number measurement due to partial volume effect.

The RFA system consists of a 15 cm length RFA electrode (Cool-tip, Covidien, USA) powered by impedance-controlled RF generator (RF Ablation System, Medtronic, USA), a peristaltic pump (B Braun Medical, Malaysia) that circulate chilled 0.9% saline solution (NaCl) and a grounding pad that was pasted at the bottom of the stainless-steel tray to close the loop circuit [3]. A medical spinal needle (22G x 3.5”), consisting of a stylet needle with a button-head in a sheath tube, was next inserted through the liver sideward to guide the insertion of the fiber optics temperature sensor. The liver sample was positioned under a 128-slice CT scanner (Siemens SOMATOM Definition AS, Germany).

After the alignment of the spinal needle, the stylet needle was withdrawn to facilitate insertion of a fiber optic of 15 μm diameter. It comprised 4 Fiber Bragg Grating (FBG) sensors, each spaced 1 cm apart along the fiber optic. The closest FBG position was at 1 cm away on the left of the center of the RFA applicator. The FBG sensors were chosen because unlike Type-K thermocouples, they do not cause

metal streaking artefact. The FBGs had a calibration range of 20˚C to 200˚C with a thermal sensitivity of 9.2 pm/˚C. A laser generator was connected to a laser interrogator which transmitted light of wavelength in the range of 1520 to 1580 nm to the gratings in the liver tissues. A change in temperature at the grating position during thermal ablation or cooling would result a change in wavelength. The final wavelength was reflected back to the interrogator and recorded in the data logger software (Bayspec, USA). Figure 1 shows the schematic diagram of the experimental setup.

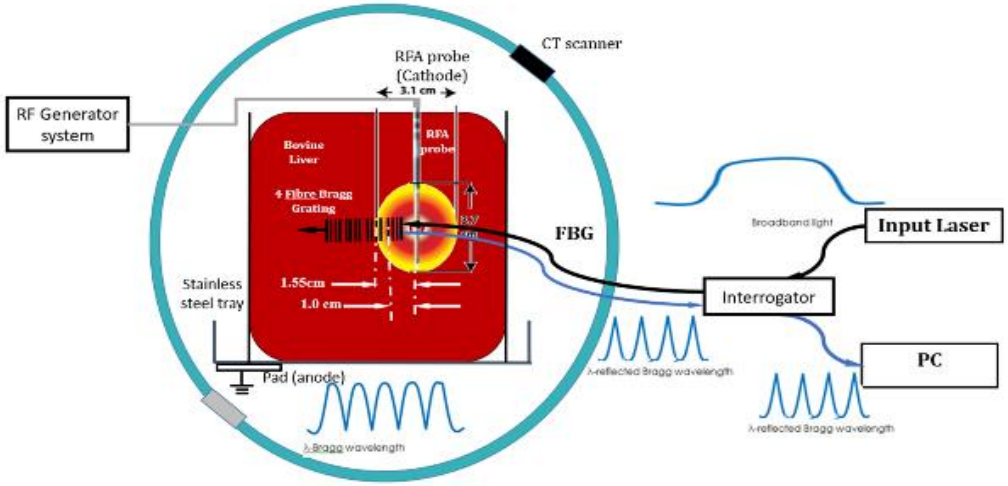

Figure 1. Schematic diagram of CT-guided RFA on ex-vivo bovine liver using an optical fiber with 4 FBG sensors.

2.2. RFA and CT Scan

The RFA system was set based on the recommended parameters for hepatic tumor ablation which delivered 480 ± 9.6 kHz. RF energy to the Cool-tip electrode that would yield an ablation size of 3.1 to 3.6 cm (horizontal diameter) and 3.7 cm (vertical diameter) in 12 minutes. The RFA system was set to manual mode so that the RF power could be manually increased every 1 minute from 25 W to 100 W. Impedance-controlled mode was used and the ablation was automatically stopped after 12 minutes.

CT scan was acquired every 3 minutes while ablation and cooling were ongoing. The CT scan parameters are as following: 120 kVp, 50 mAs, 1 mm slice thickness, 512 x 512 matrix size, B30f convolution reconstruction kernel.

2.3. Data analysis

The CT images corresponding to the location of the fiber optic were selected and analyzed. 4 regions-of-interest (ROIs), each with a circular area of 0.5 cm^2 was manually drawn at the FBG positions at 1, 2, 3 and 4 cm away from the central axis of the RFA probe. The CT numbers of the 4 ROIs were manually extracted from each scanning time. The readings were subtracted with the original CT number at time = 0 to obtain dHU. The subtractions were repeated 3 times to obtain a mean dHU and standard deviation on each FBG position at each scan time. For 10 sets of experiments, a total of 400 dHU were computed and plotted against dT.

3. Results and Discussion

3.1. Temperature Measurement from the FBG Sensors

Figure 2 shows the temperature plots of the 4 FBGs. The temperature recorded by FBG 1 raised rapidly within 8 minutes and reached steady temperature around 70˚C. There was smaller rise in temperature recoded by FBG 2, 3 and 4 as these FBGs were positioned further away from the ablated zone. After RF power was cut off at 12 minutes, the temperature of FBG 1 decreased transiently while the temperature

of FBG 3 and 4 rose steadily below necrosis temperature. The continued rise in temperature could be due to heat conduction away from the coagulated ablated zone.

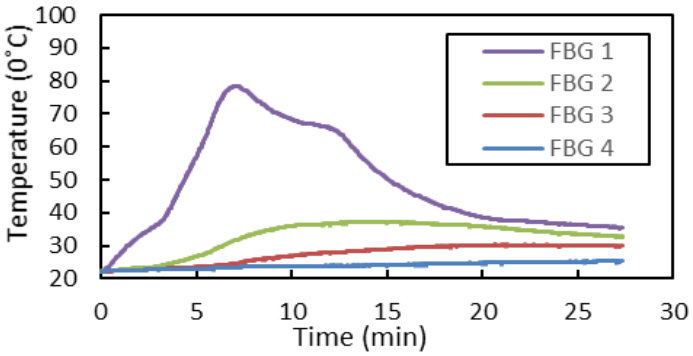

Figure 2. Plots of temperature measured by the 4 FBGs.

3.2. Correlation of CT Number with Tissue Temperature

Figure 3 shows the correlation between the changes of CT number (dHU) and the changes of tissue temperature (dT). Similar to previous studies [13-17], CT number decreased as tissue temperature increased. A negative linear regression line was plotted and the determinant of coefficient, R2 was found to be 0.925, indicating that a linear model is a good fit for HU-temperature relationship. Thermal sensitivity is represented by the gradient of the dHU/dT plot. Similar to the results of previous studies [9-13], the thermal sensitivity obtained from this study was -0.66 ± 0.03 HU/˚C.

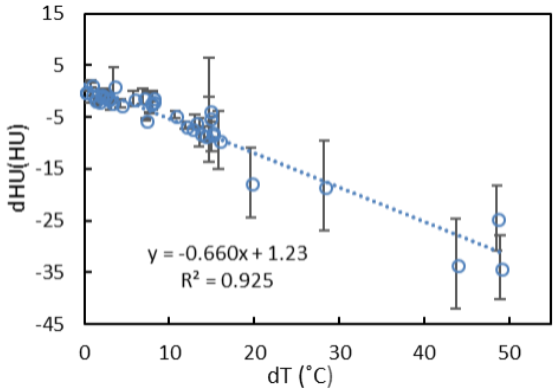

Figure 3. Correlation of CT number changes (dHU) with the changes of tissue temperature (˚C).

3.3. Contactless thermometry: CT-based thermal map

The equation y = -0.66x + 1.23 (Figure 3) is corresponding to:

$$dHU = -0.66\ (dT) + 1.23 \quad (1)$$

$$HU(x,y)_{Tfinal} - HU(x,y)_{T0} = -0.660\ (T-T_0)\ dT \quad (2)$$

$$T = \frac{HU(x,y)_{T_{final}} - HU(x,y)_{T_0}}{-0.660} + T_0 \quad (3)$$

where $HU(x,y)_{Tfinal}$ is the CT number (Hounsfield Unit) after RFA, and $HU(x,y)_{T0}$ is the CT number (Hounsfield Unit) before RFA.

Equation (3) forms the basis of CT thermometry whereby the tissue temperature at each pixel can be estimated based on the changes on the CT number. A 2-D and even 3-D thermal maps can therefore be developed with the help of software, as illustrated in Figure 4. The use of CT-based thermal maps

not only provides an invaluable visual tool for interventionalists to estimate the tissue temperature during ablation, it can also be used as an aid for interventionalists in their assessment on the dimensions of the tissues that have been ablated. Therefore, it is expected that through this method, the efficacy of thermal ablations can be improved and that the probabilities of leaving residual lesion tissues after a thermal ablation can be reduced.

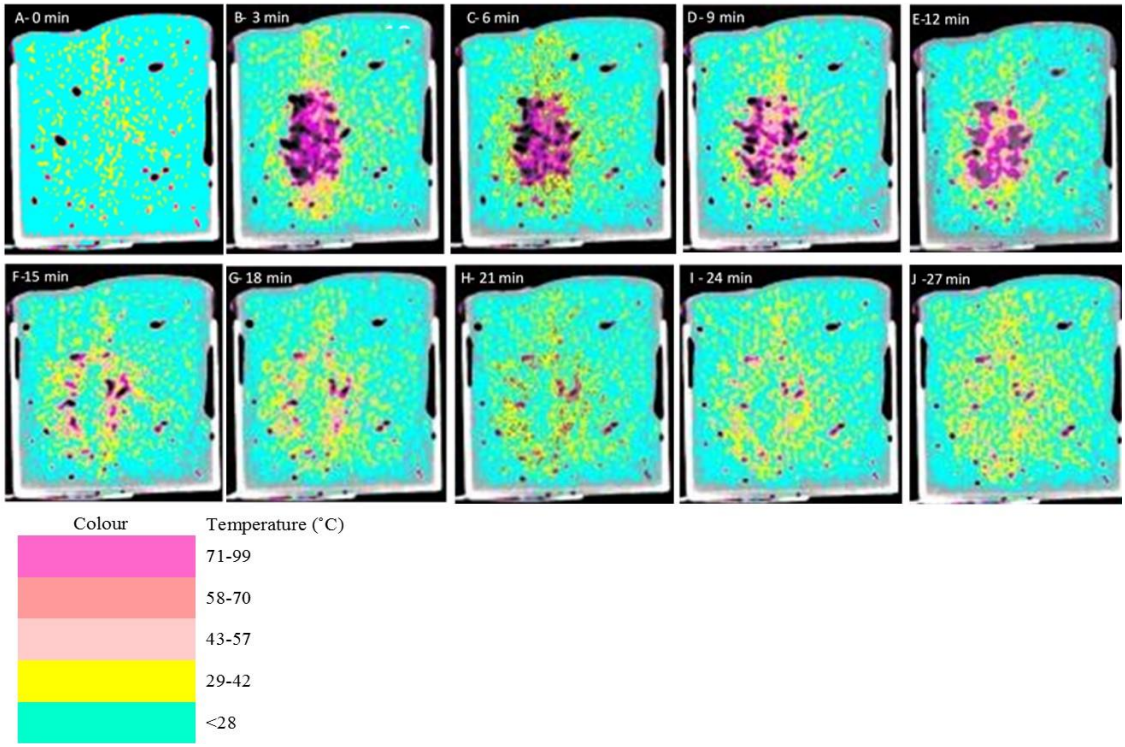

Figure 4. CT-based thermal maps that aids visualization of the tissue temperature during RFA.

4. Conclusion

This study shows a strong negative correlation between changes of CT number and tissue temperature during RFA of ex-vivo bovine samples. This finding is in agreement with the studies carried out by Pandeya et al [9,13]. These findings can potentially lead to the development of contactless 2D CT-based thermal maps that can be used as a non-invasive tool to aid interventionalists in determining the adequacy of ablation and hence improve treatment outcome.

5. References

[1] Lau, Stephanie H. Y, Wan Y.L and Lai, Eric C. H. 2016 Initial Clinical Assessment and Patient Selection, in: Chen, M, Wan Y.L, Zhang Y. *Radiofrequency ablation for small hepatocellular carcinoma*, Dordrecht: Springer, pp. 25–38.

[2] Zhou. Z and Chen M 2016 Percutaneous radiofrequency thermal ablation, in: Chen, M, Wan Y.L, Zhang Y. *Radiofrequency ablation for small hepatocellular carcinoma*, Dordrecht: Springer, pp. 39–46.

[3] Zhang Y 2016. Radiofrequency ablation systems and operating mechanisms, in Chen, M, Wan Y.L, Zhang Y. *Radiofrequency ablation for small hepatocellular carcinoma*, Dordrecht: Springer, pp 25-34

[4] Tatli S, Tapan U, Morisson P.R, Silverman 2012. *Radiofrequency ablation: technique and clinical applications*, Diagn Interv Radiol, vol 18, pp 508-16:

[5] Hong K and Georgiades Christos 2010. *Radiofrequency ablation: mechanism of action and devices*, J Vasc Interv Radiol, vol 21, pp 179-186

[6] Chu, K.F and Dupuy, D.E 2014. *Thermal ablation of tumours: biological mechanism and advances in therapy*, Nature reviews-cancer, vol 14., pp 199-208
[7] Park M.Y, Jung S.E, Cho S.H, Piao X.H and Hahn S.T 2009. *Preliminary experience using high intensity focused ultrasound for treating liver metastasis from colon and stomach Int J Hyperthermia*, vol 25, pp 180-8
[8] Fukushima T, Ikeda K, Kawamura Y, Sorin Y, Hosaka T, Kobayashi M, Sitoh S, Sezaki H, Akuta, N, Suzuki F, Suzuki Y, Arase Y, Kumada 2015. *Oncology*, vol 89, pp 47-52
[9] Pandeya G.D, Klaessns J.H.G.M, Greuter M.J.W, Schmidt B, Flohr T, Hillegersberg R.van and Oudekerk 2011. *Feasibility of computed tomography-based thermometry during interstitial laser heating in bovine liver*, Eur Radiol, vol 21, pp 1733-38
[10] Saccomandi P, Schena E, Massaroni, Fong Y, Grasso R.F. Giurazza F, Beomonte Z, Buy X, Palussiere J, Cazzato R.L 2015 *Temperature monitoring during microwave ablation in porcine livers*, Eur. J. Surg. Oncol., vol. 41, pp 1699-1705
[11] Schena, E, Giuraza F, Massaroni C, Fong Y, Park J.J and Saccomandi P 2017. *Thermometry based on computed tomography images during microwave ablation: trials on ex vivo porcine liver*, IEEE pp 1-6
[12] Bruners P, Pandeya G.D, Levit E, Rosesch E, Penzkofer T, Isfort P, Schmidt B, GreuterM.J.W Oudkerk M, Schmitz-rode T, Kuhl C.K and Mahnken A.H 2012. *CT-based temperature liver, monitoring during hepatic RF ablation: feasibility in an animal model*, Int.J. Hyperthermia, vol 28, issue, pp 55-61
[13] Pandeya G D, Greuter M.J.W,Koert P.d.J, Schmidt B, Flohr T and Oudkerk M 2011. *Feasibility of noninvasive temperature assessment during radiofrequency liver ablation on computed tomography*, J Comput Assist Tomogr, vol 35, pp 356-60.
[14] Schena E, Tosi D, Saccomandi P, Lewis E and Kim T 2016. *Fiber optic sensor for temperature monitoring during thermal treatments: An overview*, MDPI, sensors, vol 16, issue1144, pp 1-20
[15] Tosi, D, Macchi G, Braschi G, Gallati M, Cigada A, Poeggel G, Leen G and Lewis E 2014. *Monitoring of radiofrequency thermal ablation in liver tissue through fiber bragg grating sensors array*, Electron Lett, vol 50, pp 981-3